

Fig. 1. Schematic diagram of flash evaporated deposition reactor.



Fig. 2. Surface morphology of $(\text{Bi}_2\text{Te}_3)_{0.2}(\text{Sb}_2\text{Te}_3)_{0.8}$ compounds powders by SEM.

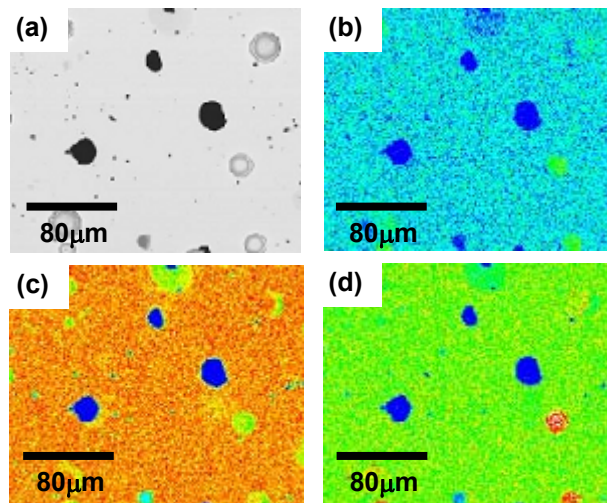


Fig. 3. SEM and X-ray map of micrograph obtained on as-grown $(\text{Bi}_2\text{Te}_3)_{0.2}(\text{Sb}_2\text{Te}_3)_{0.8}$ compounds thin films by flash evaporated deposition. Image is shown in (a), Bi in (b), Te in (c), Sb in (d).

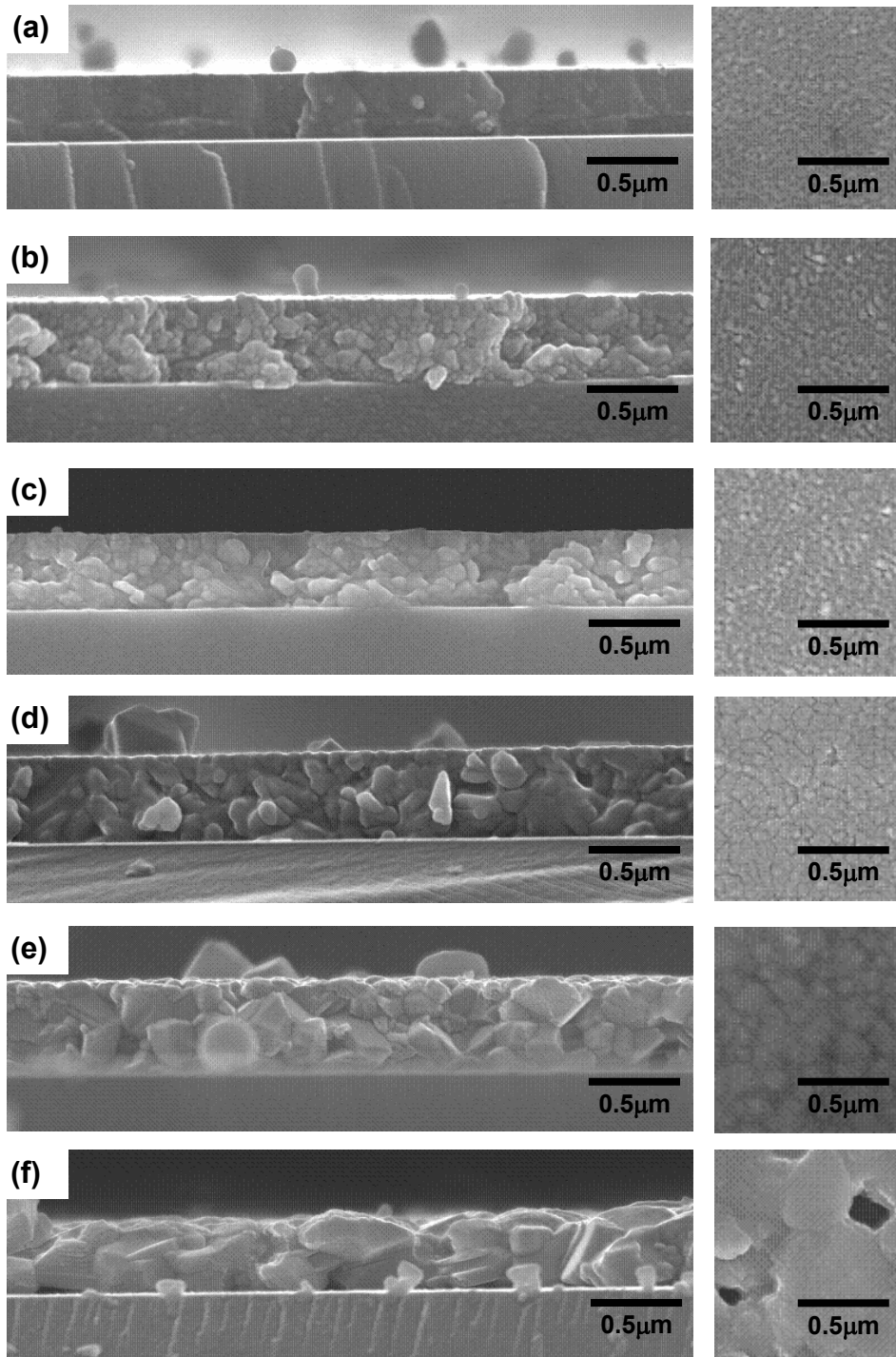


Fig. 4. Cross-section and surface micrograph on $(\text{Bi}_2\text{Te}_3)_{0.2}(\text{Sb}_2\text{Te}_3)_{0.8}$ compounds thin films by flash evaporated deposition. As-grown thin film is shown in (a), annealing temperature at 200°C in (b), 250°C in (c), 300°C in (d), 350°C in (e), 400°C in (f).

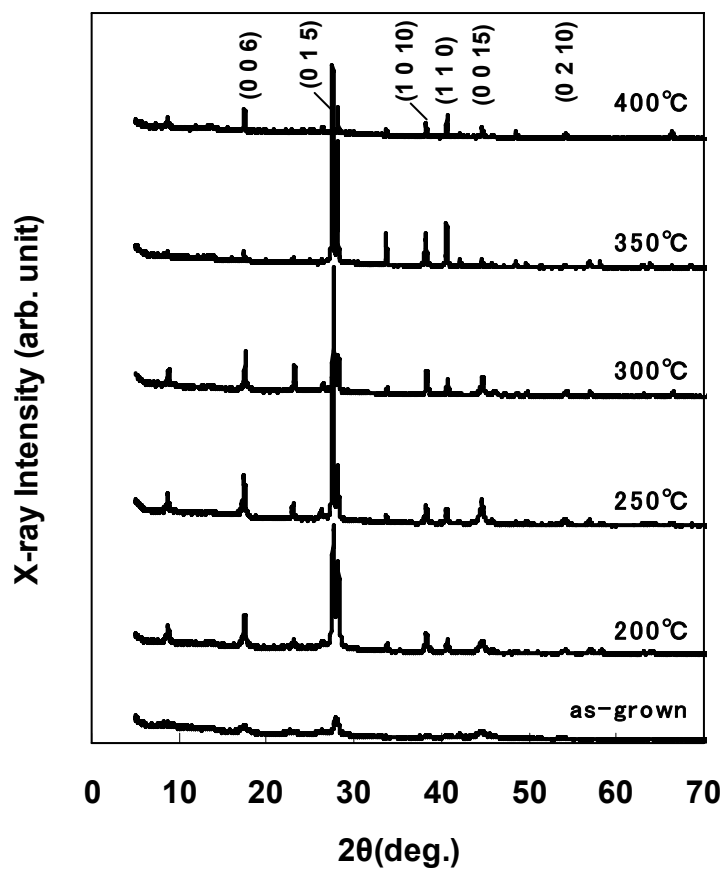


Fig. 5. X-ray diffraction patterns of $(\text{Bi}_2\text{Te}_3)_{0.2}(\text{Sb}_2\text{Te}_3)_{0.8}$ compounds thin films by flash evaporated deposition.

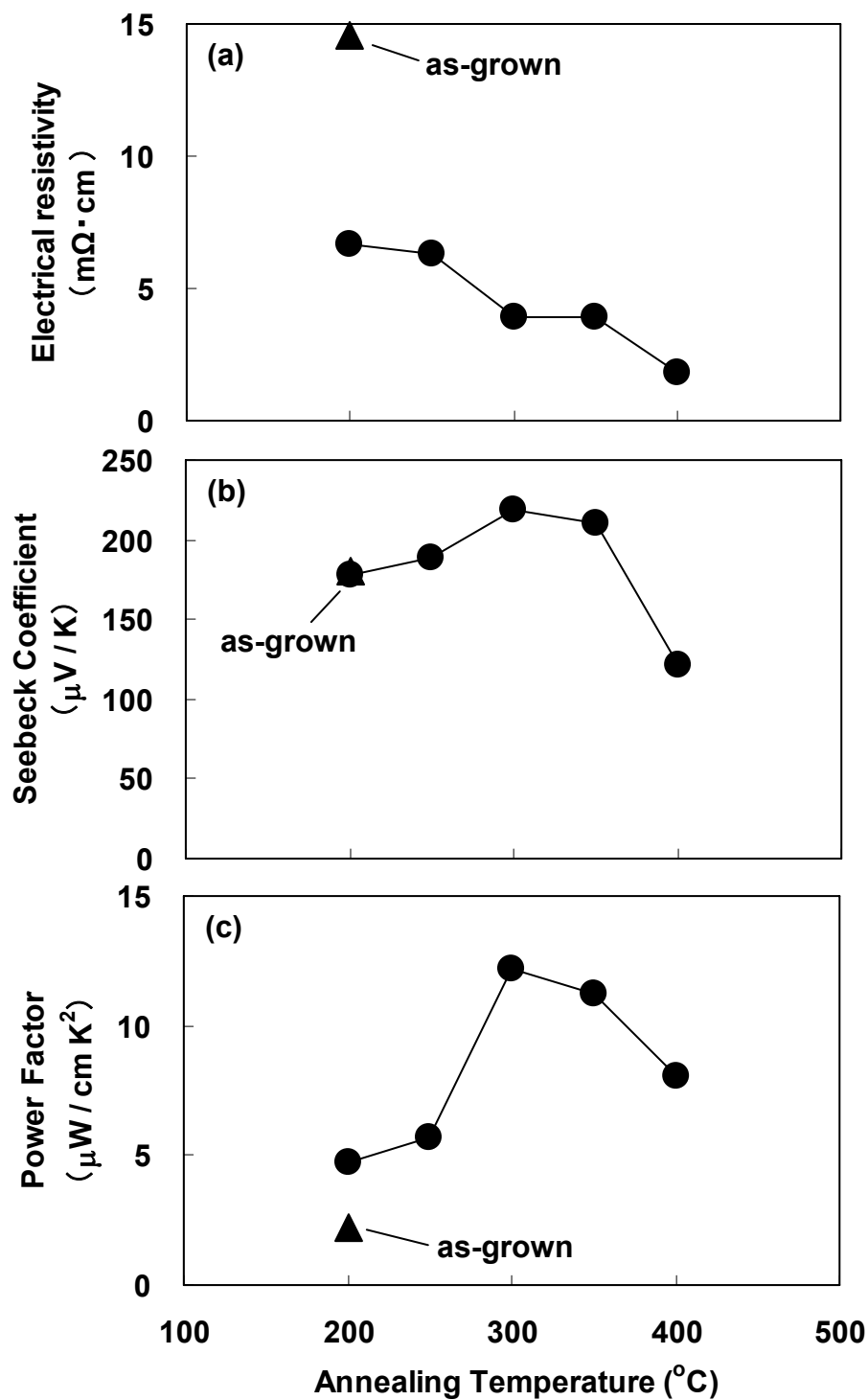


Fig. 6. Annealing temperature dependence of transport properties on $(\text{Bi}_2\text{Te}_3)_{0.2}(\text{Sb}_2\text{Te}_3)_{0.8}$ compounds thin films by flash evaporated deposition. Electrical resistivity is shown in (a), Seebeck coefficient in (b), power factor in (c).